J. He, X. Huang, X. Ning, T. Zhou, J. Wang, R. Yuan (2020) *Stairwell smoke transport in a full-scale high-rise building: influence of opening location*, **Fire Safety Journal**, 103151. doi: 10.1016/j.firesaf.2020.103151

Stairwell smoke transport in a full-scale high-rise building: Influence of opening location

Junjiang He[a,c], Xinyan Huang[b] , Xiaoyao Ning[a], Tainnian Zhou[a], Jian Wang [a*], Richard Yuan[c]

[a] State Key Laboratory of Fire Science, University of Science and Technology of China, Hefei, Anhui 230026, PR China

[b] Department of Building Services Engineering, Hong Kong Polytechnic University, Hong Kong, PR China

[c] Department of Architecture and Civil Engineering, City University of Hong Kong, Hong Kong, PR China

Abstract

In this study, a series of experiments were conducted with varying number of pool fires and opening locations (floors with ventilation openings) in a 21-story full-scale office building to study the transport phenomena and stratification of hot smoke in the stairwell. The experiments show that the flame of the pool fire inclines away from the side lobby door as pushed by the side air entrainment. The strength of stack effect in the stairwell initially increases, then decreases with the opening height increases. The rise in temperature in the stairwell can be divided into a lower and an upper region, depending on the location and attenuation effect of the upper opening. In the lower region, both the stack effect and turbulent mixing play important roles in the movement of hot smoke, in contrast, in the upper region, turbulent mixing dominates. The equivalent heat release rate for hot smoke in the upper region is determined through theoretical analysis, and an integrated correlation is proposed for predicting the rise time of the smoke plume in the stairwell. These unique full-scale experiments in a high-rise building provide crucial experimental data and empirical correlations that help the design of safer smoke ventilation systems for stairwells.

Keywords: Full-scale experiment; Smoke ventilation; Temperature distribution; Empirical correlation

Nomenclature

Symbols		u	airflow velocity (m s^{-1})
A	sectional area of the shaft (m^2)	U	smoke plume velocity (m s^{-1})
C	constant for smoke travel time	V	volume flow rate (m^3 s^{-1})
C_p	specific heat (kJ kg^{-1} K^{-1})	W	width of the stairwell (m)
d	length of shaft cross-section (m)	z	height above the fire source (m)
D	shaft hydraulic diameter (m)		
D_{th}	thermocouple diameter (m)	**Greeks**	
g	gravity acceleration (m s^{-2})	α	fitting constant
h	convective coefficient (W m^{-1} K^{-1})	β	temperature attenuation coefficient
H	height of the shaft (m)	γ	fitting constant for travel time
H_u	opening height (m)	ρ	density of the hot smoke (kg m^{-3})
k	thermal conductivity (W m^{-1} K^{-1})	$\Delta\rho$	density difference (kg m^{-3})
L	length of the stairwell (m)	σ	Stefan–Boltzmann constant (W m^{-2} K^{-4})
$\dot{m}$	mass loss rate (kg s^{-1})	ξ	emissivity (-)
Nu	Nusselt number	μ	dynamic viscosity (kg s^{-1} m^{-1})
Pr	Prandtl number	η	correction coefficient
Q	heat release rate (kW)		
Q^*	nondimensional HRR	**Subscript**	
Q_u^*	equivalent upper HRR	a	ambient air
Ri	Richardson number	e	ethanol
S	area of the lobby door (m^2)	l	lower region
t	lower smoke travel time (s)	O_2	oxgen
t'	upper smoke travel time (s)	s	shaft
T	temperature (K)	TC	thermocouple
ΔT	temperature difference (K)	u	upper region

1. Introduction

In recent years, fire accidents in high-rise buildings have occurred more frequently and caused several casualties and significant loss of property [1]. Statistics show that nearly 85% of the deaths were caused by toxic smoke from the fire [2, 3]. There are many vertical shafts in high-rise buildings, such as stairwells, elevator shafts, ventilation shafts, and cable shafts. In the event of a fire, these vertical shafts become the primary passages by which smoke spreads to other floors [4-6]. The stairwell, in particular, is a crucial evacuation channel for people; however, it allows the smoke to spread rapidly and, more importantly, poses a serious threat to their safety. Therefore, it is of great significance to study the mechanisms of smoke movement in the stairwells of high-rise buildings. Stack effect and turbulent mixing are the two primary physical mechanisms that drive the vertical rising motion of buoyant smoke flowing through a stairwell [7, 8]. Stack effect is a phenomenon caused by the pressure difference between the gas inside the stairwell and the air outside of the stairwell [7], while turbulent mixing is a phenomeon connected with Rayleigh-Taylor instability [9, 10].

A number of small-scale studies have been conducted to investigate the transport of thermal smoke in high-rise buildings. Marshall [11] explored smoke movement using 1/5 scale model of a five-story open shaft and proposed an empirical equation for predicting the air entrainment in the shaft. Cannon and Zukoski [12] studied turbulent mixing in a vertical shaft using saltwater/water experiments and obtained a turbulent mixing equation. The equation utilizes the Boussinesq approximation, which approximates the ratio of the rising smoke density to the air density. Based on Cannon and Zukoski's study, Cooper [13] further investigated smoke movement and developed a turbulent mixing equation. Tanaka et al. [14] conducted a set of experiments investigating the time taken for the smoke plume to rise in free space and vertical shafts and summarized the relationship between the travel time and the smoke plume front. Shi et al. [15] studied the influence of the stack effect on fire behavior in a room adjacent to a stairwell. The results show that the flame tilt angle increased by Ri^{-1}, and the airflow velocity at the bottom opening was proportional to 1/3 power of heat release rate (HRR) of fire source. Li et al. [16] studied the position of the neutral plane using a 1/3 scale stairwell with three openings and found that the neutral plane was influenced by the height of the middle opening. Zhao et al. [17] used the Fire Dynamics Simulator (FDS), version 6.0.1, to investigate fire-induced smoke movement in a 1/3 scale stairwell and obtained simulation results that are in overall good agreement with experimental data from Li's study. Ji et al. [18-22] conducted a series of small-scale experiments to study the effect of the stairwell ventilation state and opening height on smoke movement and temperature distribution in the stairwell, and the flame characteristics in the fire room.

When fire-induced smoke flows upward in the stairwell, it is influenced by the resistance of stair treads, landing and inner walls, which can be determined using Reynolds number. However, small-scale experiments are all based on Froude modeling, which does not preserve Reynolds number. Therefore, conducting full-scale experiments is crucial for understanding the transport characteristics of thermal smoke in the stairwells of high-rise buildings. Sun et al. [23] systematically conducted full-scale experiments in an actual stairwell of height 27 m, and combined these with numerical simulations to study smoke movement mechanisms in a closed stairwell. Peppes et al. [24, 25] conducted a series of experiments to study the smoke mass tansfer and heat transfer between the floors of a two-story full-scale building and provided formulas to predict these two phenomena. They then extended their findings to a three-story residential building. Hadjisophocleous et al. [26] conducted numerical simulations investigating smoke movement in a 10-story full-scale tower and discussed comparisons of the results derived with their model and those of previous experiments [27]. Qin et al. [28] numerically investigated smoke movement and ambient airflow in a typical two-story confined stairwell and found a fairly distinct region of hot smoke and ambient air under different fire scenarios. Li et al. [29] conducted a set of full-

scale simulations investigating the transport phenomena of fire-induced smoke flow in a semi-open vertical shaft and the results show that thermal plumes were pushed away from the center of the shaft by entrained airflow because one side of the shaft was open.

In an open stairwell with an upper opening that is not located at its top, the stairwell will be divided into two regions. The lower region, which has an upper and a bottom opening, can be regarded as an open stairwell, while the upper region with only a bottom opening is regarded as a closed stairwell. A previous study found that there are only turbulent mixing mechanisms in a closed stairwell during a fire, whereas in an open stairwell, both turbulent mixing and stack effect occur [30]. Therefore, it can be deduced that the smoke mechanisms in the lower and upper regions are different. Moreover, the height of the upper opening connecting the stairwell to the outside may also impact the transport characteristics of thermal smoke in the stairwell [22]. However, only a little attention has been devoted to transport phenomena and smoke stratification for different opening heights in a full-scale stairwell.

Therefore, to investigate the characteristics and stratification of a rising thermal plume, experiments were carried out in a 21-story full-scale stairwell in an office building. The HRR of a pool fire and the opening locations, i.e., the floor with an opening (opening floor), in the stairwell were varied in these experiments. Fire behavior and the distribution of smoke temperature and velocity were also investigated to establish a series of empirical correlations.

2. Full-scale experiments

Eight full-scale experiments were conducted in the 21-story stairwell of an office building in Hefei, China. The layout of the stairwell and the experimental setup are shown in Fig. 1. The overall height of the stairwell is 89.7 m, with the height of the first, second, third, and 21st floors are 6 m, 4.5 m, 4.5 m, 8.4 m, respectively, while all the other floors have a height of 3.9 m. The cross section of the stairwell and lobby are 6.5 m × 2.7 m and 4 m × 2.7 m, respectively. Two doors, 2.1 m (height) by 1.4 m (width) in size, position at the middle of walls and connect the stairwell, lobby, and corridor. The experimental details are shown in Table 1.

The tests were conducted using ethanol pool fires (purity: 98%, combustion efficiency: 0.92 [31], and complete heat of combustion: 26.8 kJ/g [32]) in identical rectangular pans with dimensions of 0.585 m wide, 0.13 m high, and 0.841 m long (0.5 m^2) [33]. The fire source location was a lobby 0.8m from the stairwell door, as shown in the Fig. 2. Different numbers of pool pans were used for different HRRs of the fire source. The mass loss data on the pool fires was measured in real time using an electronic balance with a precision of 0.2 g and a sampling interval of 0.1 s. The initial mass of ethanol for each pan was 12 kg, with ±2% relative uncertainty. Two digital cameras were included in the experimental setup to record the flame shape. One was positioned at at the left side of the lobby, and the other at an angle of 30 degrees to the lobby door.

The temperature of hot smoke in the 21-floor stairwell was measured using seventy-three fine-wire K-type thermocouples (1 mm in diameter). The detailed locations of the thermocouples are shown in Fig. 2. Thirty-one thermocouples were installed in the middle of the stairwell, twenty-six thermocouples under the stair treads, and the others were installed under the landing. To account for the measuring error of these thermocouples due to radiation effect, the error between the actual hot smoke temperature and the thermocouple reading is given by [34]

$$\Delta T_{error} = T - T_{th} = \frac{\sigma \xi_{th} (1 - \xi) T^4}{h_{th} + 4\sigma \xi_{th} T^3} \quad (1)$$

$$h = \frac{Nu \cdot k}{D_{th}} = \frac{k}{D_{th}}\left[0.43 + 0.53\left(\frac{\rho U}{\mu}\right)^{0.5} Pr^{0.31}\right] \quad (2)$$

where σ is the Stefan–Boltzmann constant; ξ_{th} is the emissivity of the thermocouple. ξ is the emissivity of hot smoke; D_{th} is the thermocouple diameter, m; h_{th} is the convective heat transfer coefficient between the thermocouple and hot smoke; k is the thermal conductivity of hot smoke; ρ is the density of hot smoke; U is the velocity of hot smoke; and μ is the dynamic viscosity of hot smoke. Based on Eqs. (1) and (2), the uncertainty of these thermocouples is within 1.5 K, and the response time is less than 1 s. Three hot-wire anemometer velocity probes (Kanomax, KA12) were installed at 50 cm vertical intervals and 10 cm away from the outside of the lobby door. The measurement error of hot-wire anemometers is less than 2%.

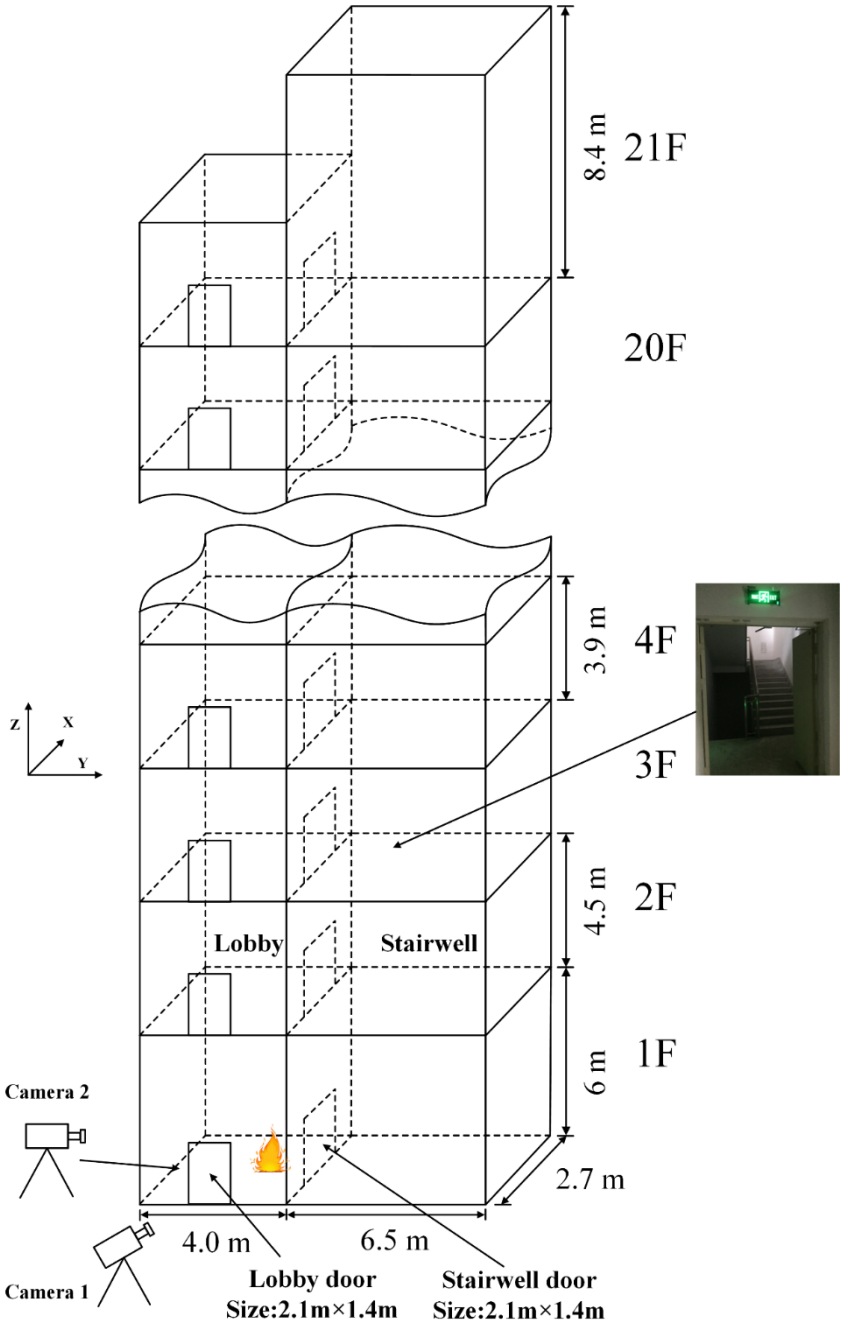

Fig. 1 Schematic of the 21-story full-scale stairwell

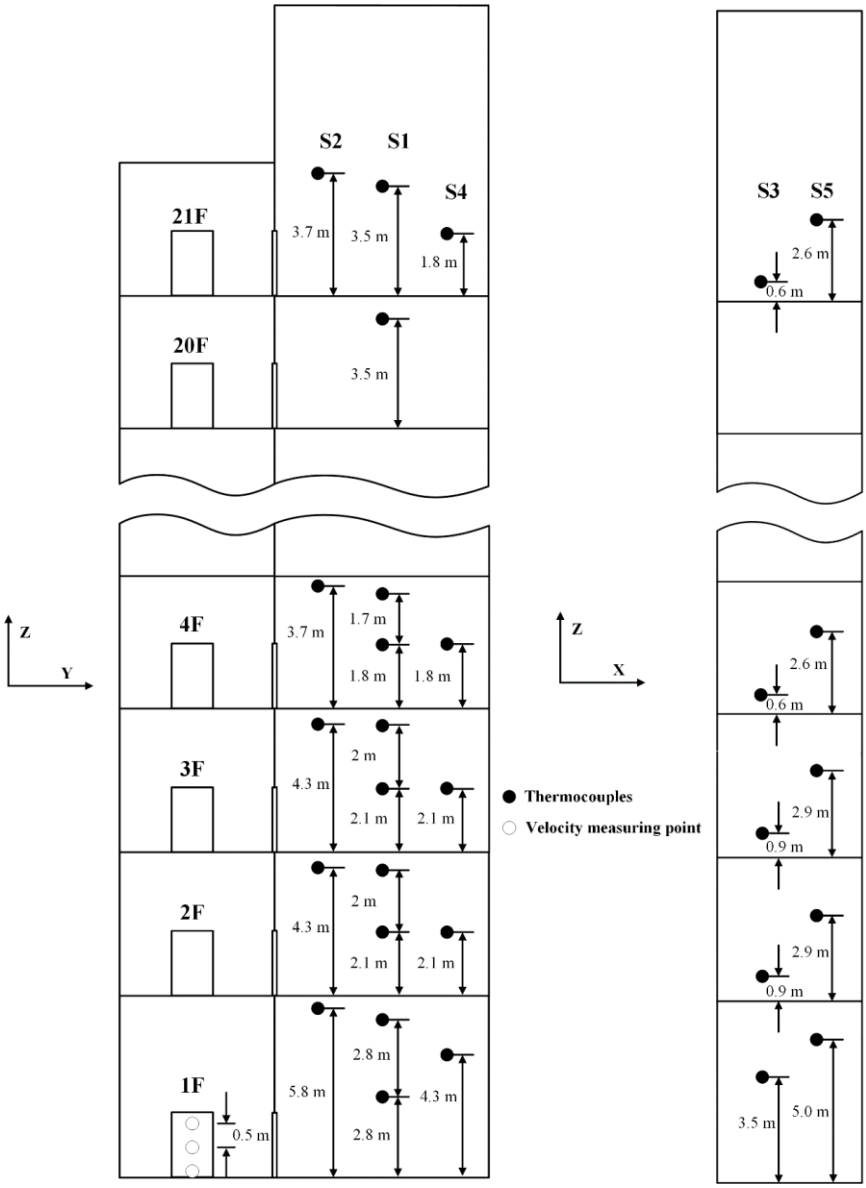

(a) Front view and right-side view

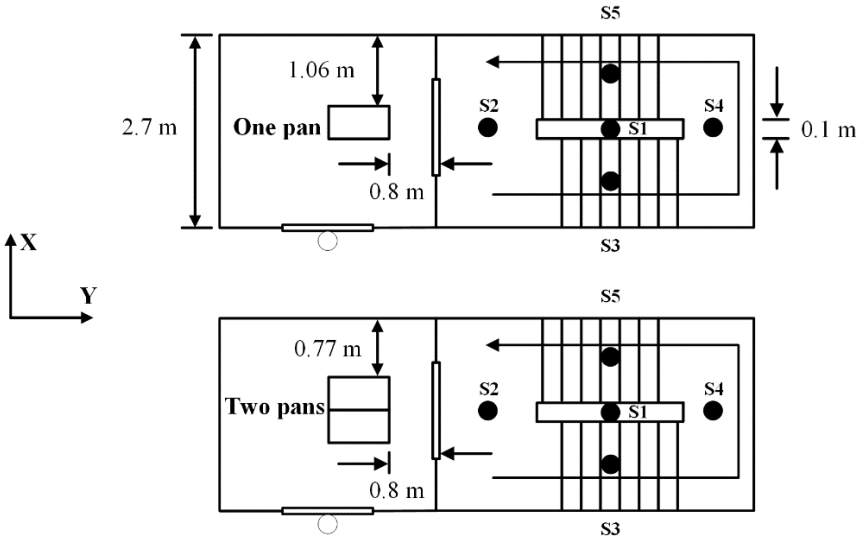

(b) Top view

Fig. 2. Locations of thermocouples and velocity measuring points.

Two doors on the first floor were kept open during the experiments, which allowed the entrainment of fresh air. In each experiment, two doors to the stairwell and lobby on the 5th, 10th, 15th, and 21st floor were left open, while other doors were kept closed and sealed during experiments to isolate the experimental space from the rest of the building. Small openings and cracks were also sealed to reduce the infiltration of outside air as much as possible. The external temperature was recorded via a mercury thermometer during each experiment, as 33–36 ℃, and the wind speed through the lobby before each experiment was 0.2–0.4 m/s. The ambient conditions remained almost constant for the entire duration of each experiment. Each experiment was repeated twice.

Table 1. Experimental details.

Case	Number of pool fires	Mass of ethanol (kg)	Opening floor
A1	1	12	5F
A2	2	24	5F
B1	1	12	10F
B2	2	24	10F
C1	1	12	15F
C2	2	24	15F
D1	1	12	21F
D2	2	24	21F

3. Results and discussion

3.1 Air flow induced by the stack effect

The flame inclination may ignite distant combustibles and enhance the probability of fire spreading in the horizontal direction. Knowledge of flame behavior has been playing an important role in fire safety design. Observing the videos from the experiments, it can be seen for the same number of pool fires, the variations in flame shapes for different heights of the opening floor (opening heights) are similar. However, the flame shapes observed are distinct for different numbers of pool fires. For example, different perspectives of a set of flame shapes over time with 15F doors open are shown in Fig. 3.

Fig. 3(a) shows the condition of one pool fire placed in the lobby, and it can be seen that in the initial stage of combustion, the flame leans slightly toward the left sidewall due to unbalanced air entrainment on both sides of the pool fire, which is induced by the open side lobby door. As the combustion progresses, increasingly more hot smoke flows into the stairwell, inducing temperature rise and the stack effect. Subsequently, the flame gradually tilts toward the stairwell due to supplement airflow through the lobby door. However, the inclination of flame skews slightly to the left at the steady stage. Comparing the flame shapes in this study to that in previous study [15], it can be seen that for this study, the ignition area is larger because the flame influences not only the front area but also the side area. When two pool fires are placed in the lobby (Fig. 3b), the volume of the flame increases as the number of pool fires increases, while the trend of the flame tilting to the left side decreases.

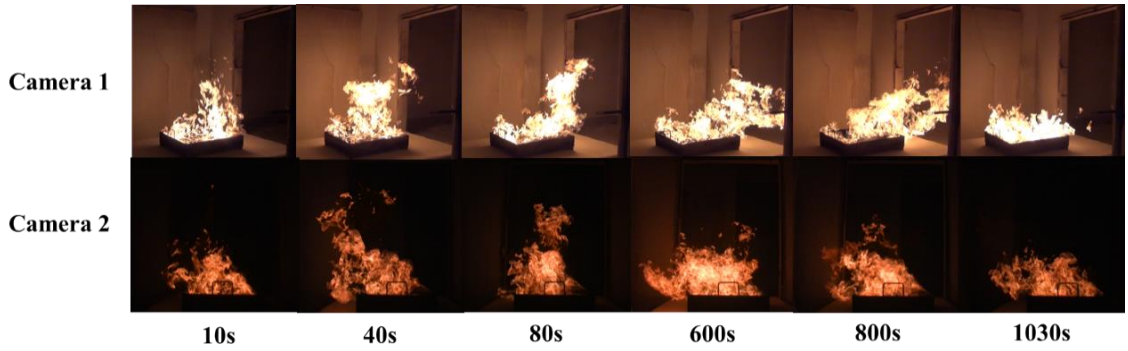

(a) 1 pool fire, doors on 15F are open

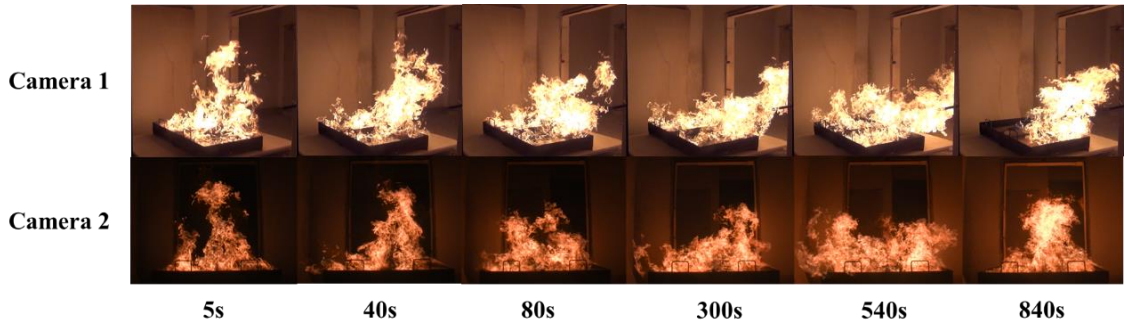

(b) 2 pool fires, doors on 15F are open

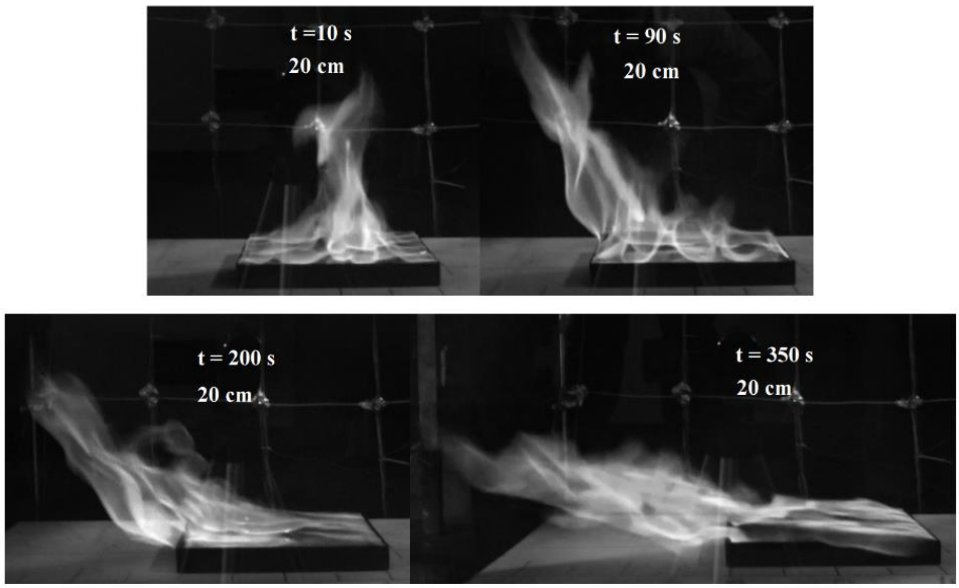

(c) Previous study [15]

Fig. 3. Flame shapes in this study and previous study

The average velocity of the air flowing into the lobby and the mass loss rate during the steady stage of combustion are presented in Fig. 4, and Table 2 presents the error bars of the velocity and mass for all cases. It can be seen that the error bars are small enough to indicate the good repeatability of the experiments. In the cases with the same opening height, the average velocity increases as the number of pool fires increases. For the same number of pool fires, the average velocity initially increases but then decreases with an increase in the opening height. This can be attributed to the magnitude of the stack effect being determined by the number of pool fires and the opening height.

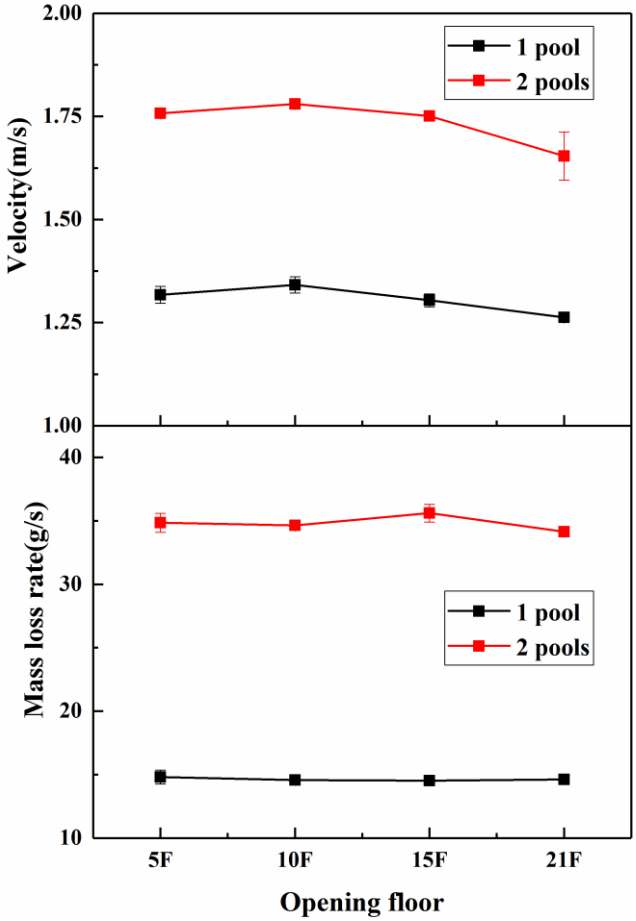

Fig. 4. Average velocity of air flowing into the lobby, and mass loss rate for all cases, during the steady stage of combustion

In an earlier study [22], the airflow velocity increased with the height of the open vent, which differs from the results of this study. A possible explanation is that the height of the building model used in that small-scale experiment is too low. The height of a small-scale stairwell is equivalent to just the 10th floor of a full-scale stairwell. Hence, the decreasing portion of the velocity curves are absent. The mass loss rate increases with the number of pool fires but remains relatively stable with changes in opening height, indicating that the mass loss rates for different ventilation conditions are almost the same.

Table 2. Average value and error bar of the velocity and mass.

Case	Velocity (m/s)		Mass (g/s)	
	Average value	Error bar	Average value	Error bar
A1	1.32	0.020	14.8	0.548
A2	1.76	0.006	34.9	0.747
B1	1.34	0.019	14.6	0.092
B2	1.78	0.010	34.6	0.097
C1	1.30	0.016	14.5	0.130
C2	1.75	0.011	35.6	0.698
D1	1.26	0.005	14.6	0.221
D2	1.65	0.058	34.1	0.317

3.2 Smoke temperature distribution in the stairwell

After the ignition, the fire-induced smoke flows from the lobby into the stairwell and spreads upward, resulting in a temperature rise in the stairwell. Fig. 5 shows the smoke temperature curves for the centerline of the stairwell over time in the cases of two pool fires. It can be seen from Fig. 5 that the time histories of temperature vary slightly in the cases with different opening heights. The temperature curves for the stairwell for all cases can be divided into four stages.

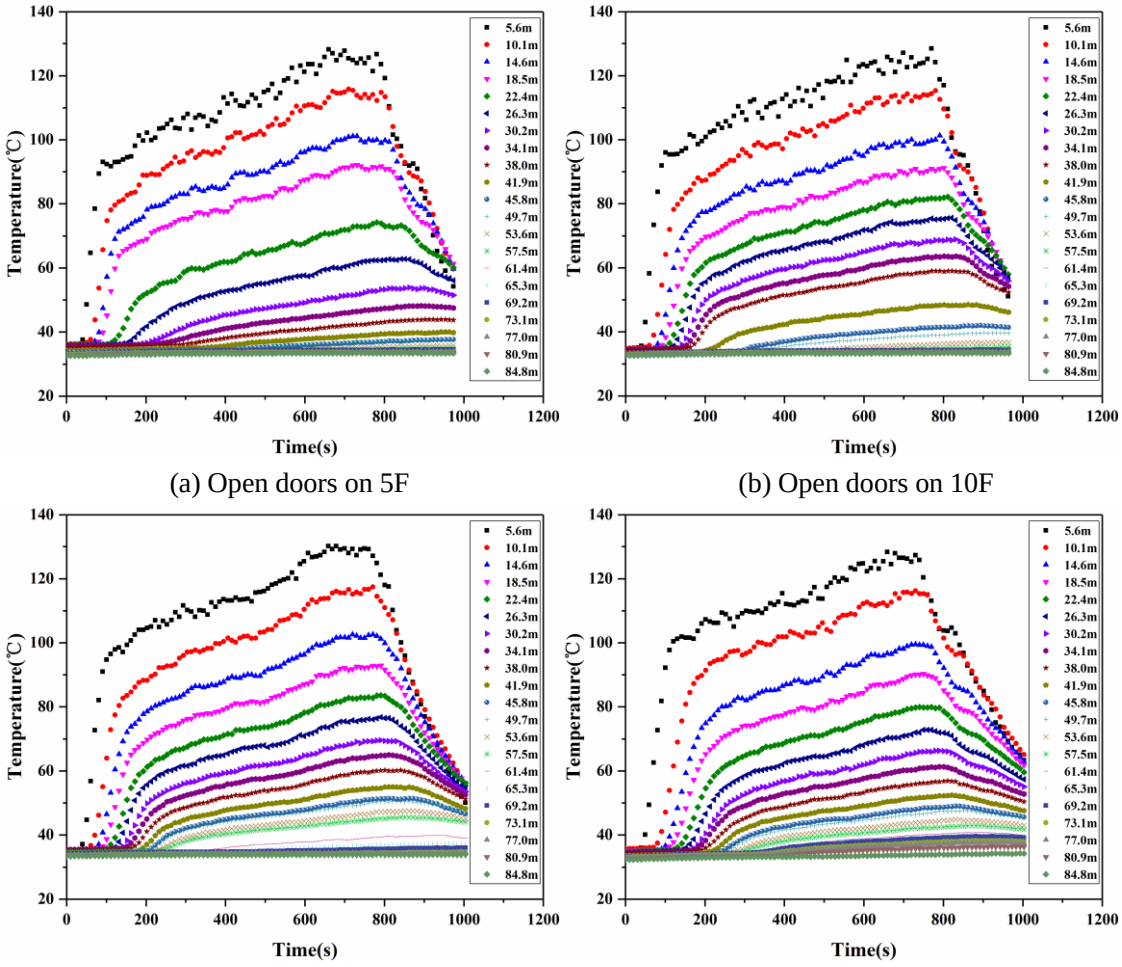

(a) Open doors on 5F (b) Open doors on 10F

(c) Open doors on 15F (d) Open doors on 21F

Fig. 5. Smoke temperatures for the centerline of the stairwell over time in the cases of two pool fires

In the first stage, fire-induced smoke flows into the stairwell, reflected as a sharp increasing trend in the temperature curves. The second stage begins several seconds after hot smoke spreads to the upper open doors and flows out of the stairwell, and the rate of temperature rise begins to decrease. At about 650 s into the fire, the temperature in the stairwell enters the third stage (the steady stage) and remains relatively stable. At this stage, the energy exchange in the stairwell system becomes stable. Due to the burnout of fuel, the temperature proceeds to the fourth stage and begins to decrease for about 750 s.

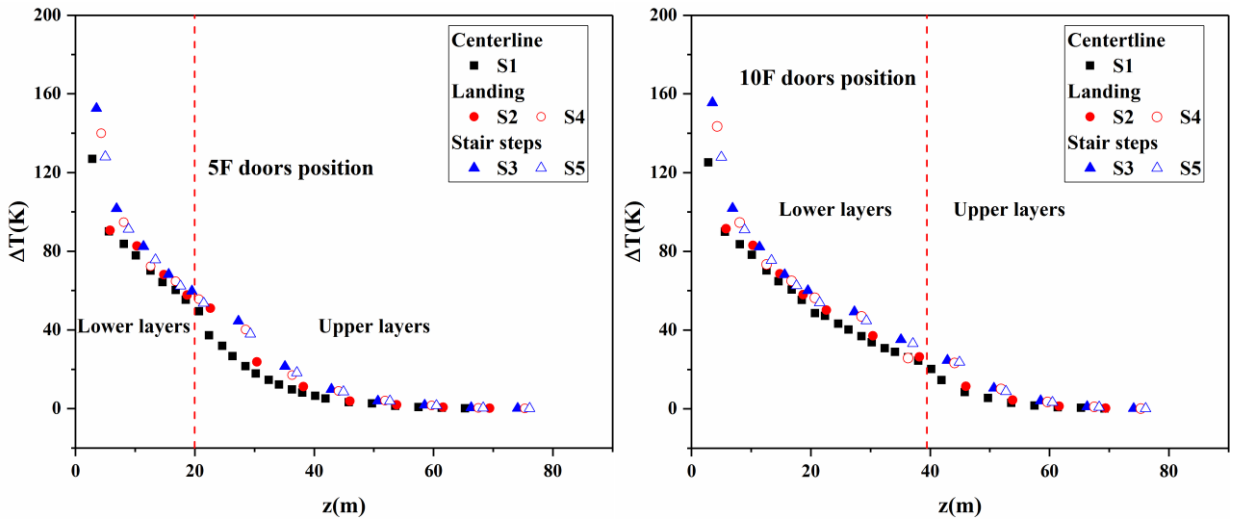

(a) Open doors are on 5F

(b) Open doors are on 5F

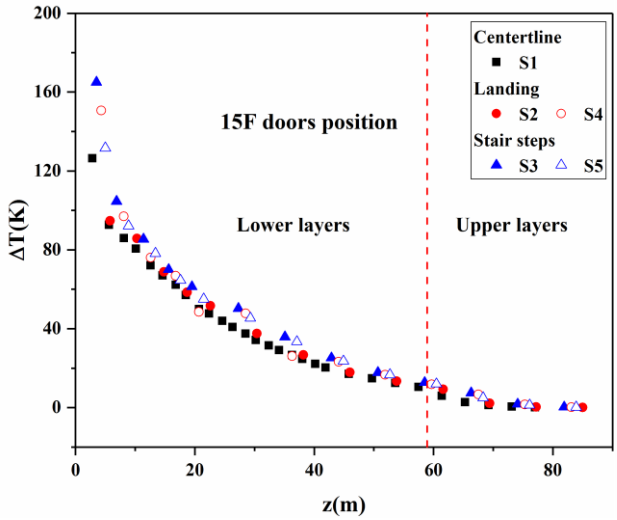

(c) Open doors are on 15F

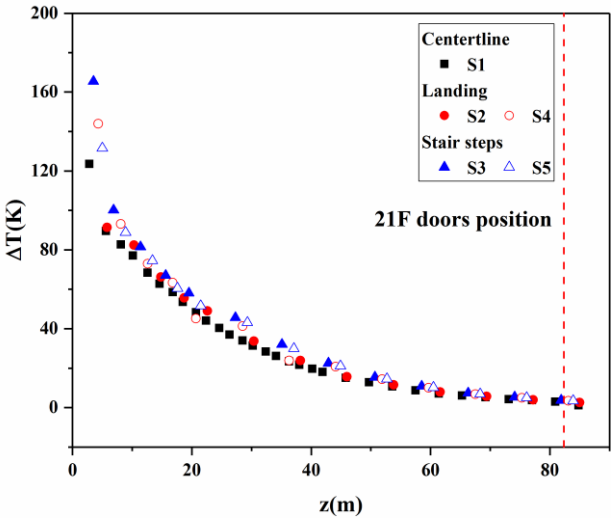

(d) Open doors are on 21F

Fig. 6. Spatial distribution of smoke temperature rise during the steady stage in cases of two pool fires.

Fig. 6 shows the spatial distribution of smoke temperature rise during the steady stage in the cases of two pool fires. The temperature rise in the stairwell decreases with height during the steady stage, and the temperature rise distribution curve for the stairwell can be divided into two parts: a lower and an upper region with different attenuation trends, by an upper opening floor. The phenomenon is caused by the different smoke movement mechanisms in the two regions. In the lower region, stack effect and turbulent mixing both play important roles in the movement of hot smoke, whereas in the upper region, only turbulent mixing plays a significant role.

Comparing the smoke temperature at different positions in the stairwell, it can be seen that the temperature difference is relatively small. The smoke temperature at the centerline is slightly lower than under the landing and stair treads, which can be explained by the smoke flow pattern in the stairwell. Sun et al. observed that the smoke flow moved upward in circular patterns and formed vortices under the stair treads of each story [23]. However, there is a 10 cm wide gap between the stair treads on both sides in the full-scale stairwell. Therefore, it can be deduced that some smoke can flow through the gap to an upper story, as shown in Fig. 7, resulting in the temperature difference.

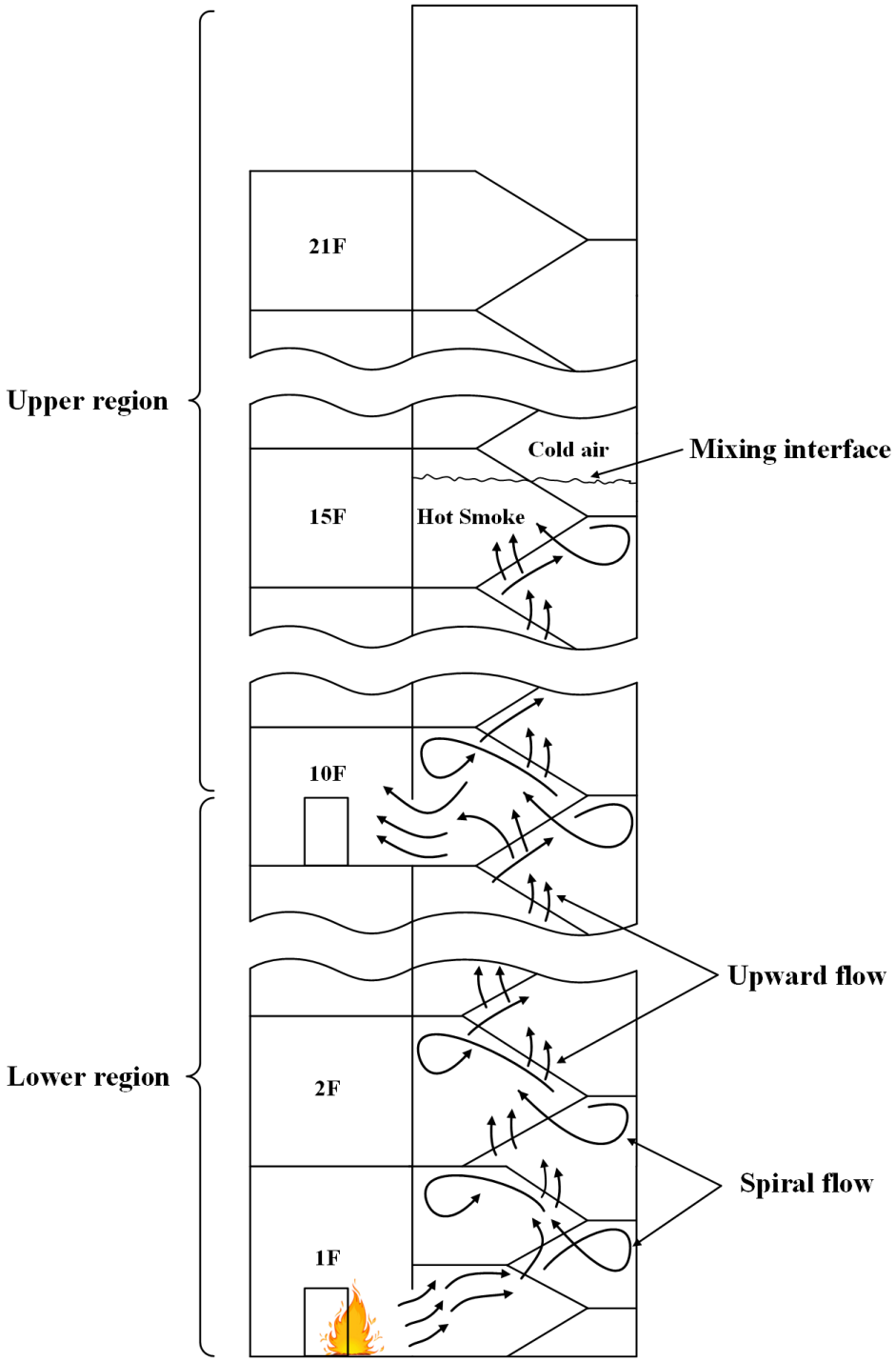

Fig. 7. Smoke paths in the stairwell with 10F doors open

Sun et al. [35] proposed a relationship between normalized temperature rise and normalized height as follows

$$\frac{\Delta T}{T_a} = \frac{T - T_a}{T_a} = \alpha e^{-\beta \frac{z}{H}} \tag{3}$$

$$\alpha = \frac{T_f - T_a}{T_a} \tag{4}$$

$$\beta = \frac{AhH}{C_p D \dot{m}_s} \tag{5}$$

where ΔT is the temperature rise between the smoke plume and ambient air; T and T_a are the temperatures of hot smoke and ambient air; z is the height above the fire source; T_f is the temperature of the smoke plume on the fire floor; α is a constant of the smoke temperature; β is the temperature attenuation coefficient; H is the height of the shaft; A is the horizontal sectional area of the shaft; h is the convective heat transfer coefficient between hot smoke and the inner walls; D is the hydraulic diameter of the shaft; and $\dot{m}_s$ is the mass flow rate in the shaft.

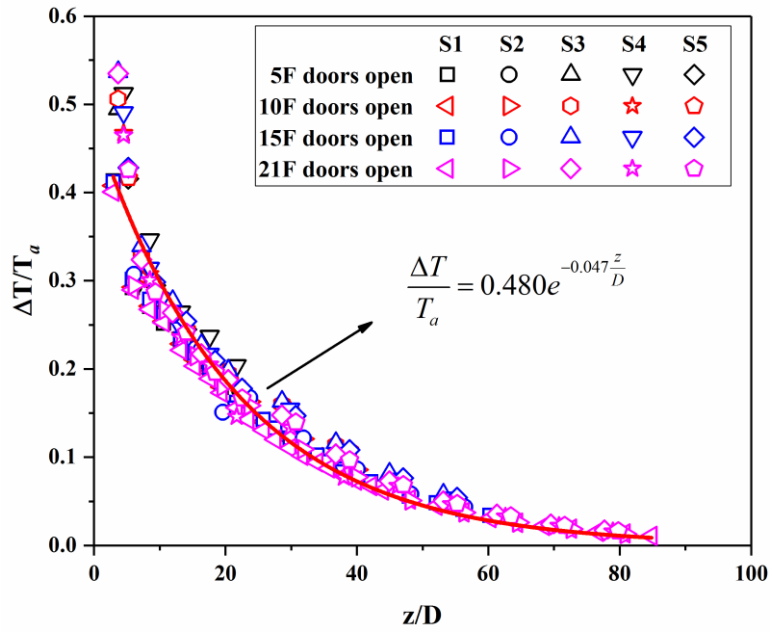

(a) Lower region

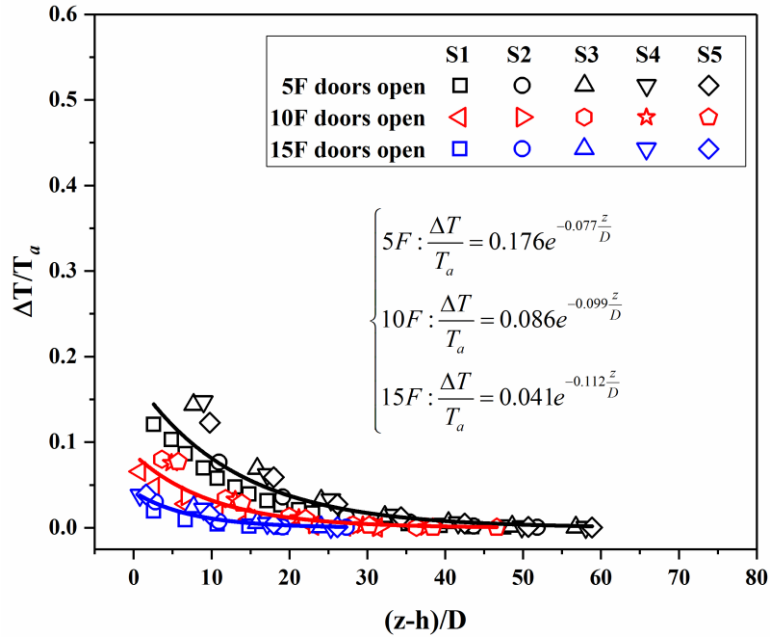

(b) Upper region

Fig. 8. Normalized temperature rise vs. normalized height during the steady stage in cases of two pool fires

In the experiments conducted in this study, the height H in Eqs. (3) and (5) is replaced with the hydraulic diameter D of the stairwell [19], which is given by

$$D = \frac{L \times W}{2(L + W)} \tag{6}$$

where L is the length (6.5 m) and W is width (2.7 m) of the stairwell. Therefore, we can derive

$$\frac{\Delta T}{T_a} = \alpha e^{-\beta \frac{z}{D}} \tag{7}$$

$$\beta = \frac{Ah}{C_p \dot{m}_s} \tag{8}$$

The relationship between normalized temperature rise and normalized height in the cases of two pool fires is presented in Fig. 8, and Eq. (7) was used to fit the temperature data. As shown in Fig. 8, in the lower region, the temperature data for different opening heights can be fitted by a curve. This indicates that the opening height has only little influence on the temperature distribution of hot smoke in the lower region. In contrast, the fitted temperature curves for the upper region become steeper with increasing opening height. The fitted values of β are summarized in Table 3.

As shown in Table 3, β decreases with an increasing number of pool fires for the same opening height due to a larger value of $\dot{m}_s$ in the cases of two pool fires. Because thermal smoke flows out through the upper doors, resulting in a decrease of $\dot{m}_s$ for the upper region, β in the lower region is smaller than that in the upper region. In the upper region, β decreases with opening height becasuse the amount of hot smoke flowing into the upper region gradually decreases with increasing opening height.

Table 3. Fitted values of β in all cases.

Number of pool fires	Lower region	Upper region		
		5F	10F	15F
1	0.052	0.083	0.100	0.113
2	0.047	0.078	0.099	0.112

3.3 Smoke rise time in stairwell

Tanaka [14] posited that the temperature for a given height would rise sharply due to contact with a rising smoke plume. Based on this method, the time for the plume front to get to the centerline thermocouples for all cases can be obtained, as shown in Fig. 9. On the fire floor, the precise rise time for the plume front is affected by flame pulsations due to strong air entrainment. Therefore, data from thermocouples on the fire floor are neglected. For the cases with the same opening height, the smoke plume front can reach a higher position as the number of pool fires increases. For the same number of pool fires, the maximum height that the smoke plume can reach also increases with the opening height. It can be also seen that the rising velocity of the smoke plume is distinct in the upper region and lower region. For the lower region, the height-time curve is an approximately straight line, indicating that the rising velocity is an almost fixed value due to a balance between the stack effect, turbulent mixing, and block effect of the stair treads. However, the height-time curve for the upper region is a parabola, which indicates that the rising velocity gradually decreases with increasing height due to the turbulent mixing in the hot smoke having less influence than the block effect from the stair treads and the pressure effect of the fresh air in the upper region.

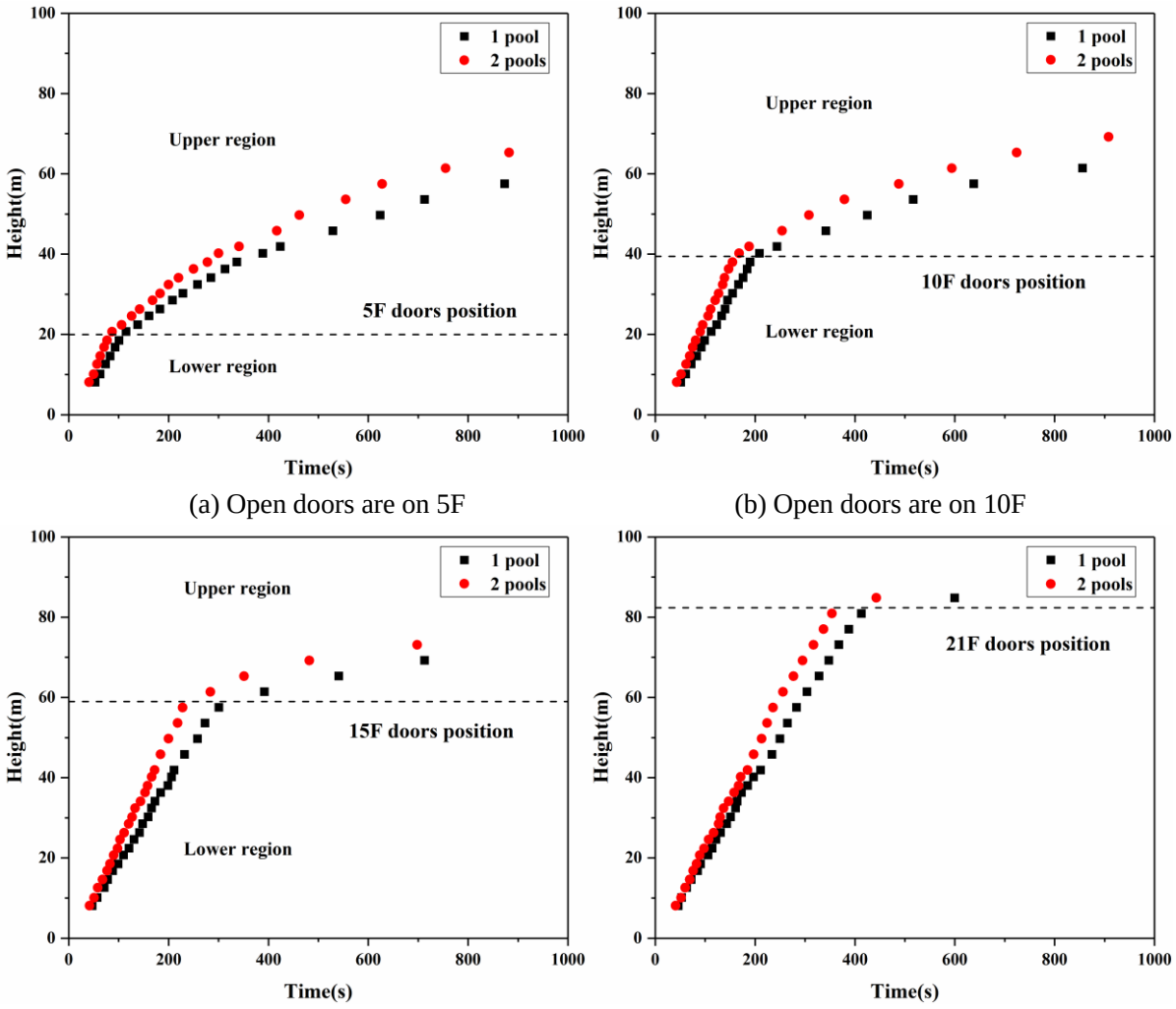

(a) Open doors are on 5F

(b) Open doors are on 10F

(c) Open doors are on 15F

(d) Open doors are on 21F

Fig. 9. Increasing heights of the rising smoke plume front vs time, for all cases

Tanaka [14] assumes that the heat transfer from a fire plume to the surrounding walls is insignificant, and proposed an empirical model that expresses the relationship between the increasing of time and the increasing height of the plume as follows

In open shaft

$$t\sqrt{\frac{g}{d}}(Q^*)^{\frac{1}{3}} = \begin{cases} 0.56\left(\frac{z}{d}\right)^{\frac{4}{3}} & \left(\frac{z}{d} \le 5\right) \\ 1.64\left(\frac{z}{d}\right)^{\frac{2}{3}} & \left(\frac{z}{d} > 5\right) \end{cases} \tag{9}$$

In closed shaft

$$t\sqrt{\frac{g}{d}}(Q^*)^{\frac{1}{3}} = \begin{cases} 0.56\left(\frac{z}{d}\right)^{\frac{4}{3}} & \left(\frac{z}{d} \le 2.5\right) \\ 0.30\left(\frac{z}{d}\right)^{2} & \left(\frac{z}{d} > 2.5\right) \end{cases} \tag{10}$$

$$Q^* = \frac{Q}{C_p \rho_a T_a \sqrt{g} d^{\frac{5}{2}}} \tag{11}$$

where t is the travel time of a smoke plume front from the fire source to a given height; is the density of ambient air; Q is the HRR of the fire source; and d is the side length of the shaft cross section.

In the experiments in this study, the hydraulic diameter D given by Eq. (6) is taken as the characteristic length of the stairwell. The time t can be expected to be a function of the height of the smoke plume front, the characteristic length of the stairwell, gravity and the HRR of the fire source as follows

$$t\sqrt{\frac{g}{D}}(Q^*)^{\frac{1}{3}} = C\left(\frac{z}{D}\right)^{\gamma} \tag{12}$$

where C and γ are constants of smoke travel time.

If stoichiometric burning occurs in the lobby, the overall chemical reaction of the pool fire can be expressed as

$$2\ C_2H_5OH + 7\ O_2 \rightarrow 4\ CO_2 + 6\ H_2O$$

Therefore, the relationship between the rate of oxygen consumption and the mass loss rate of ethanol can be expressed as

$$\dot{m}_{O_2} = 3.5\dot{m}_e \tag{13}$$

where $\dot{m}_{O_2}$ is the rate of oxygen consumption, and $\dot{m}_e$ is the mass loss rate of ethanol. Because 21% of air is oxygen, the ratio of the air entrainment rate to the rate of oxygen consumption can be expressed as

$$\frac{\dot{m}_a}{\dot{m}_{O_2}} = \frac{\rho_a V_a}{\rho_{O_2} V_{O_2}} = \frac{\rho_a}{0.21\rho_{O_2}} = 4.31 \tag{14}$$

where ρ_a and ρ_{O_2} are the density of air and oxygen, and V_a and $V_{O_2}$are the volume of air and oxygen. Substituting Eq. (14) into Eq. (13) gives

$$\dot{m}_a = 15.09\dot{m}_e \tag{15}$$

It can be concluded that burning 1 kg of ethanol requires 15.09 kg of air for stoichiometric burning to occur. In this study, the air entrainment rate can be expressed as follows

$$\dot{m}_a = \rho_a S u \tag{16}$$

where S is the area of the lobby door and and u is is the velocity of the airflow through the lobby door.

Table 4. Entrainment rate of air and mass loss rate of ethanol.

Case	$\dot{m}_e$ (g/s)	$\dot{m}_a$ (g/s)	$\frac{\dot{m}_a}{\dot{m}_e}$
A1	14.8	5007.1	338
A2	34.9	6680.7	192
B1	14.6	5100.2	349
B2	34.6	6765.9	195
C1	14.5	4956.5	341
C2	35.6	6656.7	187
D1	14.6	4798.3	328
D2	34.1	6287.8	184

Table 4 presents the entrainment rate of air and the burning rate of ethanol. The ratios of the air entrainment rate to the ethanol burning rate for all cases are far greater than 15.09, which indicates that the combustion is fuel-controlled and the combustion coefficient are the same for all cases.

Therefore, the HRR of the fire source for all cases can be expressed as follows

$$Q = \lambda \dot{m}_e \Delta H \tag{17}$$

where λ is the combustion coefficient, 0.92. ΔH is the complete heat of combustion, 26.8 kJ/g.

As mentioned earlier, the floor with open doors divides the stairwell into two parts, a lower and an upper region. When hot smoke arrives at the opening floor, most of the smoke and heat will be vented out through the door due to the stack effect. Thus, the equivalent HRR Q_u^* for the hot smoke in upper region needs to be corrected.

For simplicity, heat transfer from a fire plume to surrounding walls was ignored, so that the HRR of the fire source can be expressed via the temperature rise and the velocity of the smoke plume as follows

$$Q \propto C_p \rho \Delta T A U \tag{18}$$

The velocity of the smoke plume can be expressed as the difference in density between the plume and ambient air, as follows

$$U \propto \sqrt{g \frac{\Delta \rho}{\rho} z} \tag{19}$$

From the ideal gas law

$$\frac{\Delta \rho}{\rho} = \frac{\rho_a}{\rho} = \frac{T - T_a}{T_a} \tag{20}$$

Substituting Eq. (20) into Eq. (19) gives

$$U \propto \sqrt{g \frac{\Delta T}{T_a} z} \tag{21}$$

Introducing the Boussinesq approximation and combining Eqs. (11), (18) and (21) gives

$$Q^* \propto \left(\frac{\Delta T}{T_a}\right)^{\frac{3}{2}} \left(\frac{A^2 z}{D^5}\right)^{\frac{3}{4}} \tag{22}$$

The correction coefficient η of the HRR for the upper region can be expressed as follows

$$\eta = \frac{Q_u^*}{Q^*} = \left(\frac{\Delta T_u}{\Delta T_f}\right)^{\frac{3}{2}} \tag{23}$$

where ΔT_u is the rise in temperature between the smoke plume on the opening floor and ambient air and ΔT_f is the rise in temperature between the smoke plume on the fire floor and ambient air.

Combining Eqs. (3), (4) and (23) gives

$$\eta = \frac{Q_u^*}{Q^*} = e^{-\frac{3\beta H_u}{2\ D}} \tag{24}$$

$$Q_u^* = \eta Q^* = e^{-\frac{3\beta H_u}{2\ D}} Q^* \tag{25}$$

where H_u is the height from the fire source to the upper open doors. Therefore, the relationship between normalized time and normalized height can be expressed as follows

$$\begin{aligned} t\sqrt{\frac{g}{D}}(Q^*)^{\frac{1}{3}} &= C_l\left(\frac{z}{D}\right)^{\gamma_l} \quad z \le H_u \\ (t-t')\sqrt{\frac{g}{D}}(\eta Q^*)^{\frac{1}{3}} &= C_u\left(\frac{z-H_u}{D}\right)^{\gamma_u} \quad z > H_u \end{aligned} \tag{26}$$

where t' is the travel time for a smoke plume front from the fire source to the upper open doors; C_l, C_u, γ_l, and γ_u are constants of smoke travel time.

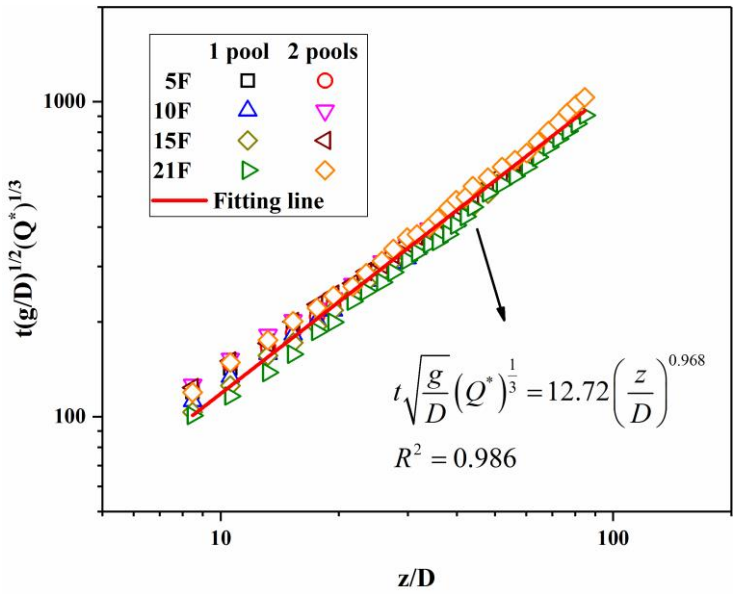

(a) Lower region

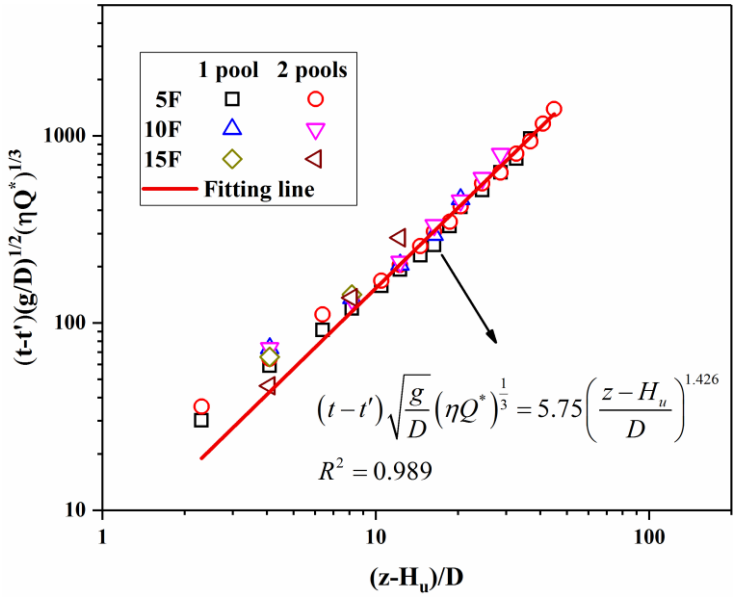

(b) Upper region

Fig. 10. Relationship between normalized rise-time and normalized height in the stairwell

Fig. 10 shows the relationship between normalized time and normalized height. The experimental results are well fitted with Eq. (26), which has correlation coefficients are greater than 0.98. A comparison of the coefficient γ for the full-scale experiment with those for a few previous studies is presented in the

Table 5. It can be seen that the coefficient γ in the open condition is smaller than in that the closed condition. Because of the block effect of the stair treads, the coefficient γ for the stairwell is larger compared to that for the shaft, indicating lower velocity of hot smoke in the stairwell. While in a closed condition, the coefficient γ for the full-scale stairwell are smaller than that for the shaft. This is because the movement of the upper smoke in the full-scale stairwell is boosted by the lower smoke, leading to an increase in velocity. The comparison of the coefficient γ for the full-scale experiments with that for some small-scale experiments shows that the resistance influencing the traveling of the smoke plume is smaller in the full-scale stairwell.

Table 5. Fitted values of γ for different studies.

Parameters	Full-scale stairwell		Small-scale stairwell[18]		Shaft[14]	
	Open (lower region)	Closed (upper region)	Open	Closed	Open	Closed
γ	0.968	1.426	1.203	2.129	0.667	2

Combining the equations in Fig. 10, the integrated correlation between normalized rise time and normalized height can be obtained as follows

$$t\sqrt{\frac{g}{D}}(Q^*)^{\frac{1}{3}} = \begin{cases} 12.72\left(\frac{z}{D}\right)^{0.968} & 6 < z \le H_u \\ 5.75\eta^{-\frac{1}{3}}\left(\frac{z-H_u}{D}\right)^{1.426} + 12.72\left(\frac{H_u}{D}\right)^{0.968} & z > H_u \end{cases} \quad (27)$$

Where $\eta = e^{-\frac{3\beta H_u}{2\ D}}$. A comparison of the experimentally measured normalized rise time and the calculated normalized rise time using Eq. (27) was conducted, and the linear regression analysis is presented in Fig. 11. The results show that Eq. (27) provides good predictions for the rise time of the smoke plume front, and the maximum error is less than 20%.

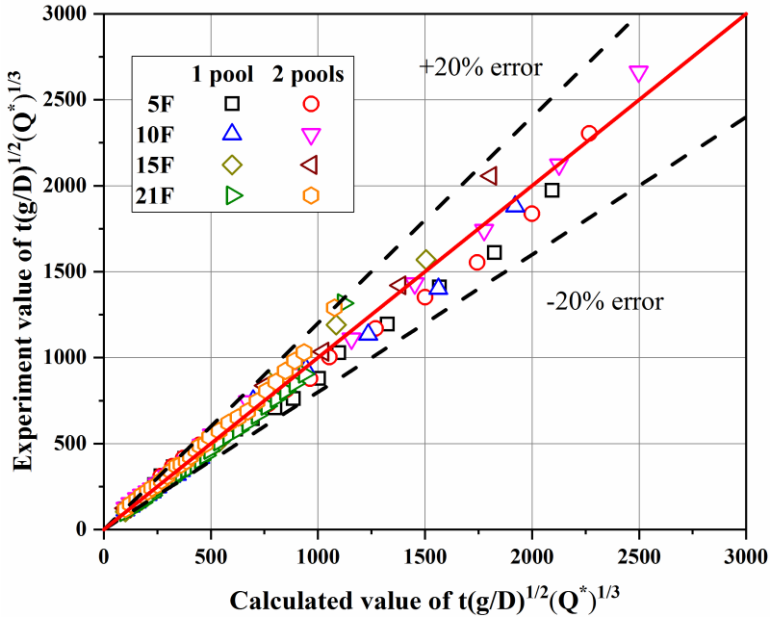

Fig. 11. Comparison of the experimentally measured and the calculated values using Eq. (27)

4. Conclusion

In this study, a series of full-scale experiments were carried out with varying heat release rates and varing opening locations (floors with ventilation openings) to study the transport phenomena and stratification of hot smoke in a stairwell.

The experiments show that the flame of the pool fire inclines away from the side lobby door, as it is pushed by the side air entrainment. The strength of stack effect initially increases, then decreases as the opening height increases. The distribution of hot smoke in the stairwell is uniform because of the stair treads. The rise in temperature of the hot smoke in the stairwell can be divided into a lower and an upper region, depending on the location and attenuation effect of the upper opening. In the lower region, both the stack effect and turbulent mixing play important roles in the movement of hot smoke, in contrast, in the upper region, turbulent mixing plays a significant role. The equivalent heat release rate for hot smoke in the upper region is determined based on theoretical analysis, and an integrated correlation is proposed for predicting the rise time of the smoke plume in the stairwell. A comparison of the coefficient γ of the full-scale and small-scale experiments indicates that resistance influenceing the traveling of the smoke plume is smaller in a full-scale experiment. These unique full-scale experiments in a high-rise building provide crucial experimental data and empirical correlations that are useful in the design of safer smoke ventilation systems for stairwells.

Acknowledgments

This work is supported by National Key R&D Program of China (No.2018YFC0809500). The authors gratefully acknowledge all of this support.

References

[1] G. Rein, 9/11 World Trade Center Attacks: Lessons in Fire Safety Engineering After the Collapse of the Towers, Fire Technology, 49 (3) (2013) 583-585.

[2] Y. Alarie, Toxicity of fire smoke, Critical reviews in toxicology, 32 (4) (2002) 259-289.

[3] A.A. Stec, T.R. Hull, Assessment of the fire toxicity of building insulation materials, Energy and Buildings, 43 (2-3) (2011) 498-506.

[4] J. Zhang, W. Lu, R. Huo, R. Feng, A new model for determining neutral-plane position in shaft space of a building under fire situation, Building and environment, 43 (6) (2008) 1101-1108.

[5] R. Priyadarsini, K. Cheong, N. Wong, Enhancement of natural ventilation in high-rise residential buildings using stack system, Energy and buildings, 36 (1) (2004) 61-71.

[6] R. Gao, A. Li, X. Hao, W. Lei, Y. Zhao, B. Deng, Fire-induced smoke control via hybrid ventilation in a huge transit terminal subway station, Energy and Buildings, 45 (2012) 280-289.

[7] J. Lee, D. Song, D. Park, A study on the development and application of the E/V shaft cooling system to reduce stack effect in high-rise buildings, Building and Environment, 45 (2) (2010) 311-319.

[8] C.H. Su, Y.C. Lin, C.M. Shu, M.C. Hsu, Stack effect of smoke for an old-style apartment in Taiwan, Building and Environment, 46 (12) (2011) 2425-2433.

[9] G.I. Taylor, The instability of liquid surfaces when accelerated in a direction perpendicular to their planes. I, Proceedings of the Royal Society of London. Series A. Mathematical and Physical Sciences, 201 (1065) (1950) 192-196.
[10] M.J. Andrews, D.B. Spalding, A simple experiment to investigate two‐dimensional mixing by Rayleigh–Taylor instability, Physics of Fluids A: Fluid Dynamics, 2 (6) (1990) 922-927.
[11] N.R. Marshall, Air entrainment into smoke and hot gases in open shafts, Fire Safety Journal, 10 (1) (1986) 37-46.
[12] J. Cannon, E. Zukoski, Turbulent mixing in vertical shafts under conditions applicable to fires in high rise buildings, Technical Fire Report no1 to the National Science Foundation, California Institute of Technology, Pasadena, California, (1975).
[13] L.Y. Cooper, Simulating smoke movement through long vertical shafts in zone-type compartment fire models, Fire Safety Journal, 31 (2) (1998) 85-99.
[14] T. Tanaka, T. Fujita, J. Yamaguchi, Investigation into rise time of buoyant fire plume fronts, International Journal on Engineering Performance-Based Fire Codes, 2 (1) (2000) 14-25.
[15] W.X. Shi, J. Ji, J.H. Sun, S.M. Lo, L.J. Li, X.Y. Yuan, Experimental study on influence of stack effect on fire in the compartment adjacent to stairwell of high rise building, Journal of Civil Engineering and Management, 20 (1) (2014) 121-131.
[16] L.J. Li, J. Ji, C.G. Fan, J.H. Sun, X.Y. Yuan, W.X. Shi, Experimental investigation on the characteristics of buoyant plume movement in a stairwell with multiple openings, Energy and Buildings, 68 (PARTA) (2014) 108-120.
[17] G. Zhao, T. Beji, B. Merci, Study of FDS simulations of buoyant fire-induced smoke movement in a high-rise building stairwell, Fire Safety Journal, 91 (2017) 276-283.
[18] J. Ji, L.J. Li, W.X. Shi, C.G. Fan, J.H. Sun, Experimental investigation on the rising characteristics of the fire-induced buoyant plume in stairwells, International Journal of Heat and Mass Transfer, 64 (2013) 193-201.
[19] J. Ji, M. Li, Y. Li, J. Zhu, J. Sun, Transport characteristics of thermal plume driven by turbulent mixing in stairwell, International Journal of Thermal Sciences, 89 (2015) 264-271.
[20] J. Ji, H. Wan, Y. Li, K. Li, J. Sun, Influence of relative location of two openings on fire and smoke behaviors in stairwell with a compartment, International Journal of Thermal Sciences, 89 (2015) 23-33.
[21] J. Ji, M. Li, Z.H. Gao, Y.F. Li, W.X. Shi, J.H. Sun, Experimental investigation of combustion characteristics under different ventilation conditions in a compartment connected to a stairwell, Applied Thermal Engineering, 101 (2016) 390-401.
[22] J. Ji, M. Li, W. Shi, Z. Gao, J. Sun, S. Lo, Deflection characteristic of flame with the airflow induced by stack effect, International Journal of Thermal Sciences, 115 (2017) 160-168.
[23] X.Q. Sun, L.H. Hu, Y.Z. Li, R. Huo, W.K. Chow, N.K. Fong, G.C.H. Lui, K.Y. Li, Studies on smoke movement in stairwell induced by an adjacent compartment fire, Applied Thermal Engineering, 29 (13) (2009) 2757-2765.
[24] A.A. Peppes, M. Santamouris, D.N. Asimakopoulos, Buoyancy-driven flow through a stairwell, Building and Environment, 36 (2) (2001) 167-180.

[25] A.A. Peppes, M. Santamouris, D.N. Asimakopoulos, Experimental and numerical study of buoyancy-driven stairwell flow in a three storey building, Building and Environment, 37 (5) (2002) 497-506.
[26] G. Hadjisophocleous, Q. Jia, Comparison of FDS prediction of smoke movement in a 10-Storey building with experimental data, Fire Technology, 45 (2) (2009) 163-177.
[27] Y. Wang, A study of smoke movement in multi-storey buildings using experiments and computer modelling, Carleton University, 2008.
[28] T. Qin, Y. Guo, C. Chan, K. Lau, W. Lin, Numerical simulation of fire-induced flow through a stairwell, Building and Environment, 40 (2) (2005) 183-194.
[29] D. Li, T. Zhou, Z. Liu, J. Wang, Transport phenomena of fire-induced smoke flow in a semi-open vertical shaft, International Journal of Numerical Methods for Heat & Fluid Flow, 28 (11) (2018) 2664-2680.
[30] W.X. Shi, J. Ji, J.H. Sun, S.M. Lo, L.J. Li, X.Y. Yuan, Influence of fire power and window position on smoke movement mechanisms and temperature distribution in an emergency staircase, Energy and Buildings, 79 (2014) 132-142.
[31] A.P. Hamins, J.C. Yang, T. Kashiwagi, Global model for predicting the burning rates of liquid pool fires (NISTIR 6381), in, 1999.
[32] D. Rakopoulos, C. Rakopoulos, R. Papagiannakis, D. Kyritsis, Combustion heat release analysis of ethanol or n-butanol diesel fuel blends in heavy-duty DI diesel engine, Fuel, 90 (5) (2011) 1855-1867.
[33] A. Standard, AS 4391-1999 Smoke Management Systems–Hot Smoke Test, Standards Association of Australia, (1999).
[34] M. Luo, Effects of radiation on temperature measurement in a fire environment, Journal of Fire Sciences, 15 (6) (1997) 443-461.
[35] X.Q. Sun, L.H. Hu, W.K. Chow, Y. Xu, F. Li, A theoretical model to predict plume rise in shaft generated by growing compartment fire, International Journal of Heat and Mass Transfer, 54 (4) (2011) 910-920.